Relation between the Widom line and the breakdown of the Stokes–Einstein relation in supercooled water

Pradeep Kumar, S. V. Buldyrev, S. R. Becker, P. H. Poole, F. W. Starr, and H. E. Stanley

This information is current as of June 2007.

Online Information & Services	High-resolution figures, a citation map, links to PubMed and Google Scholar, etc., can be found at: www.pnas.org/cgi/content/full/104/23/9575
References	This article cites 50 articles, 5 of which you can access for free at: www.pnas.org/cgi/content/full/104/23/9575#BIBL This article has been cited by other articles: www.pnas.org/cgi/content/full/104/23/9575#otherarticles
E-mail Alerts	Receive free email alerts when new articles cite this article - sign up in the box at the top right corner of the article or click here.
Rights & Permissions	To reproduce this article in part (figures, tables) or in entirety, see: www.pnas.org/misc/rightperm.shtml
Reprints	To order reprints, see: www.pnas.org/misc/reprints.shtml

Notes:

Relation between the Widom line and the breakdown of the Stokes–Einstein relation in supercooled water

Pradeep Kumar†‡, S. V. Buldyrev§, S. R. Becker¶, P. H. Poole‖, F. W. Starr¶, and H. E. Stanley†‡

†Center for Polymer Studies and Department of Physics, Boston University, Boston, MA 02215; §Department of Physics, Yeshiva University, 500 West 185th Street, New York, NY 10033; ¶Department of Physics, Wesleyan University, Middletown, CT 06459; and ‖Department of Physics, St. Francis Xavier University, Antigonish, NS, Canada B2G 2W5

Supercooled water exhibits a breakdown of the Stokes–Einstein relation between the diffusion constant D and the alpha relaxation time τ_α. For water simulated with two different potentials, TIP5P and ST2, we find that the temperature of the decoupling of diffusion and alpha relaxation correlates with the temperature of the maximum in specific heat that corresponds to crossing the Widom line $T_W(P)$. Specifically, we find that our results for $D\tau_\alpha/T$ collapse onto a single "master curve" if temperature is replaced by $T - T_W(P)$. We further find that the size of the mobile molecule clusters (dynamical heterogeneities) increases sharply near $T_W(P)$. Moreover, our calculations of mobile particle cluster size $\langle n(t^*)\rangle_W$ for different pressures, where t^* is the time for which the mobile particle cluster size is largest, also collapse onto a single master curve if T is replaced by $T - T_W(P)$. The crossover to a more locally structured low density liquid (LDL) as $T \rightarrow T_W(P)$ appears to be well correlated both with the breakdown of the Stokes–Einstein relation and with the growth of dynamic heterogeneities. Our results are consistent with the possibility that the breakdown of the SE relation in supercooled water at low pressures is associated with the hypothesized liquid–liquid phase transition.

liquid–liquid phase transition in water | transport properties of water | dynamic heterogeneities

An 17th century study of the density maximum at 4°C (1) demonstrates the long history of water science. Since that time, dozens of additional anomalies of water have been discovered (2–5), including the sharp increase upon cooling of both the constant-pressure-specific heat C_P and the isothermal compressibility K_T. These anomalies of water become more pronounced as water is supercooled. To explain these properties, a liquid–liquid (LL) critical point has been proposed (6). Emanating from any critical point there must be loci of extrema of thermodynamic response functions such as C_P and K_T. These loci must coincide as the critical point is approached, because response functions are proportional to powers of the correlation length, and the locus of the correlation length maxima asymptotically close to the critical point defines the Widom line $T_W(P)$ (7).

A number of other phenomena have been correlated with $T_W(P)$. Some of these phenomena are found only in experiments, such as the sharp drop in the temperature derivative of the zero-frequency structure factor or the appearance of a boson peak, both observed by quasi-elastic neutron scattering (QENS) (8). Others are found only in simulations, such as the crossover in the relaxation time of the fluctuations in orientational order parameter Q (P.K., S.V.B., and H.E.S., unpublished calculations) or the maximum in the temperature derivative of the number of hydrogen bonds per molecule (9). Finally, some anomalies that correlate with the Widom line are found in both experiments and simulations, such as the dynamic "fragile-to-strong" crossover in the diffusion constant (7, 10–12), or the sharp drop in the temperature derivative of the mean squared displacement (7, 10, 13).

In the supercooled region of the pressure–temperature phase diagram, the dynamic properties of water show dramatic changes

(14, 15). One basic relation among dynamic properties is the Stokes–Einstein (SE) relation

$$D = \frac{k_B T}{6\pi\eta a}, \qquad [1]$$

where D is the diffusion constant, T is the temperature, k_B is the Boltzmann constant, η is the viscosity, and a is the effective hydrodynamic radius of a molecule. This expression provides a relation between mass and momentum transport of a spherical object in a viscous medium. The SE relation describes nearly all fluids at $T \gtrsim (1.2–1.6)\, T_g$, where T_g is the glass transition temperature. Because the hydrodynamic radius a is roughly constant, $D\eta/T$ is approximately independent of T (16–18). However, in most liquids, for $T \lesssim (1.2–1.6)\, T_g$, $D\eta/T$ is no longer a constant (19–28). For the case of water, the breakdown of the SE relation occurs at $\approx 1.8\, T_g$, in the same temperature region in which many of the unusual thermodynamic features of water occur (5, 11, 14, 29).

Our aim is to evaluate to what degree the SE breakdown can be correlated with the presence of thermodynamic anomalies and the onset of spatially heterogeneous dynamics, and how these features relate to the location of the Widom line (22, 30–33). From prior studies of water, we can already form an expectation for the correlation between the SE breakdown and the Widom line by combining three elements: (i) the Widom line is approximately known from the extrapolated power-law divergence of K_T (34); (ii) the locus of points $T_D(P)$ where D extrapolates to zero is also known, and nearly coincides with $T_W(P)$ at low pressures (see Fig. 1 of ref. 12); (iii) the SE relation has been found to fail in liquids generally at the temperature $T_D(P)$ (35). Combining these three results, one might not be surprised if the breakdown of the SE relation should occur near to the Widom line for $P < P_C$, and it should continue to follow $T_D(P)$ for $P > P_C$. We will see that our results are consistent with this expectation, but reveal some unexpected insights.

Our results are based on molecular dynamics (MD) simulations of $N = 512$ water-like molecules interacting via the TIP5P potential (36, 37), which exhibits a LL critical point at approximately $T_C \approx 217$ K and $P_C \approx 340$ MPa (37, 38). We carry out simulations in the isothermal isobaric ensemble for three different pressures $P = 0$, 100, and 200 MPa, and for temperatures T ranging from 320 K down to 230 K for $P = 0$ and 100 MPa, and down to 220 K for 200 MPa. We also analyze MD simulations of $N = 1,728$ water-like molecules interacting via the ST2 potential
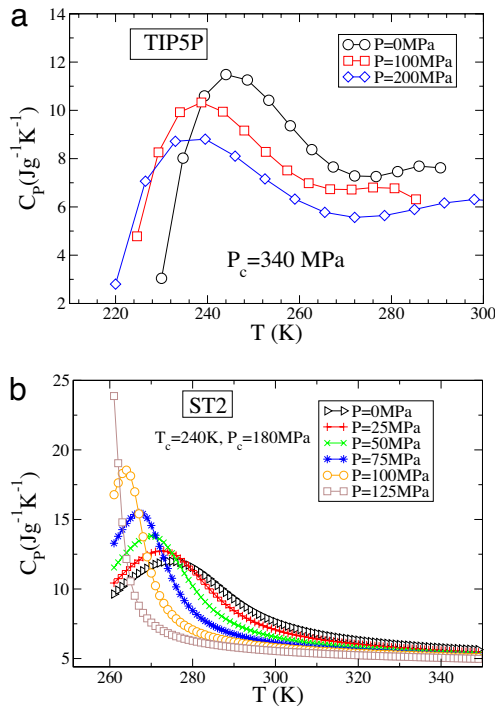
CHEMISTRY

APPLIED PHYSICAL SCIENCES

Fig. 1. Temperature dependence of C_P for the TIP5P (*a*) and ST2 (*b*) models as found from a fit of the data in ref 41 to a bicubic polynomial. Note that, in *a*, the value of $C_P(T)$ at the maximum is decreasing with increasing *P* in the range of *P* presented, which is opposite to what one would naively expect on approach to a critical point. One possible way to understand this is that, because C_P is the difference of two diverging quantities, $C_P = (dU/dT)_P - P |(dV/dT)_P|$, when $(dV/dT)_p < 0$, $C_P(T)$ is influenced by increasingly large positive and negative contributions in the region around the critical point. Reversal of the expected increase of the maximum with *P* is therefore a plausible possibility, apparently realized in the case of TIP5P. As a comparison, in ST2 water, the maximum of $C_P(T)$ does increase as *P* increases.

(39, 40), which displays a LL critical point at $T_C \approx 245$ K and $P = 180$ MPa (41). The simulations for the ST2 model are performed at fixed volume and temperature (40).

Results

We explore the possible relation between the Widom line and the breakdown of the SE relation (Eq. **1**). To locate the Widom line, we first analyze the isobaric heat capacity C_P for the TIP5P (Fig. 1*a*) and the ST2 (Fig. 1*b*) models.

We next calculate the diffusion constant via its asymptotic relation to the mean-squared displacement,

$$D \equiv \lim_{t \to \infty} \frac{\langle |\mathbf{r}_j(t) - \mathbf{r}_j(0)|^2 \rangle}{6t}, \qquad [2]$$

where $\mathbf{r}_j(t)$ is the position of oxygen *j* at time *t*. It is difficult to accurately calculate the viscosity η in simulations, so we instead calculate the alpha relaxation time τ_α (which is expected to have nearly the same *T* dependence as η) as the time at which the coherent intermediate scattering function

$$F(q, t) \equiv \frac{\langle \rho(\mathbf{q}, t)\rho(-\mathbf{q}, 0) \rangle}{\langle \rho(\mathbf{q}, 0)\rho(-\mathbf{q}, 0) \rangle}, \qquad [3]$$

decays by a factor of *e*. Here $\rho(\mathbf{q}, t) \equiv \sum_j^N \exp[-i\mathbf{q} \cdot \mathbf{r}_j(t)]$ is the Fourier transform of the density at time *t*, $\mathbf{r}_j(t)$ is the position of oxygen *j* at time *t*, **q** is a wave vector and the brackets denote an
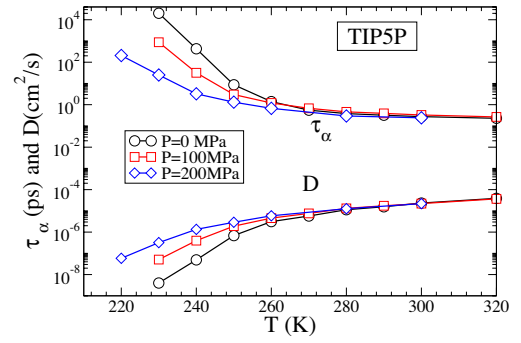
average over all $|\mathbf{q}| = q$ and many equilibrium starting configurations. We calculate $F(q, t)$ at the value of *q* corresponding to the first maximum in the static structure factor $F(q, 0)$. It is important that we use the coherent scattering function (as opposed to the incoherent, or self-scattering function), because we want to capture collective relaxation that contributes to η. We expect that τ_α calculated this way would behave similar to η and hence the SE relation (Eq. **1**) can be written as

$$\frac{D\tau_\alpha}{T} = \text{constant}. \qquad [4]$$

Fig. 2. τ_α and *D* as functions of *T* for *P* = 0, 100, and 200 MPa for the TIP5P model.
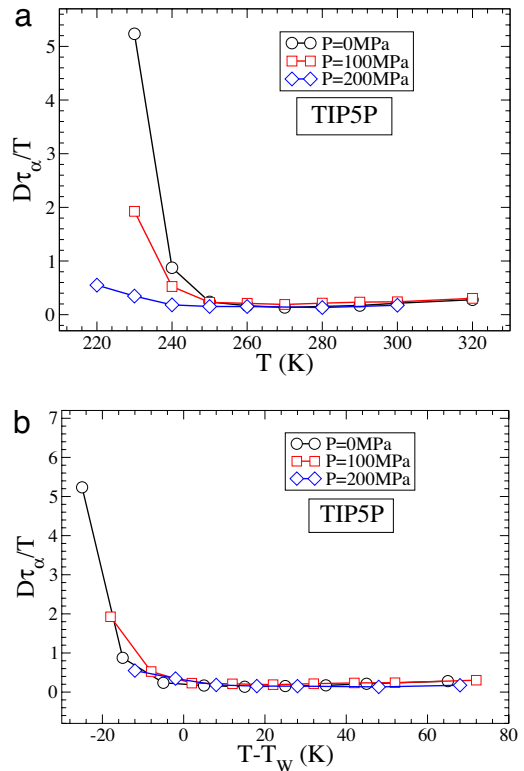

Fig. 3. Test for the TIP5P model of the key result of this paper: that the SE breakdown at low pressures is correlated with crossing the Widom line. (*a*) $D\tau_\alpha/T$ as a function of *T* for *P* = 0 MPa, 100 MPa and 200 MPa for the TIP5P model. For all panels, $D\tau_\alpha/T$ is scaled by its high *T* value to facilitate comparison of the different systems. (*b*) $D\tau_\alpha/T$ as a function of $T - T_W(P)$ for TIP5P. The curves for different pressures overlap on the same master curve when *T* is replaced by $T - T_W(P)$.
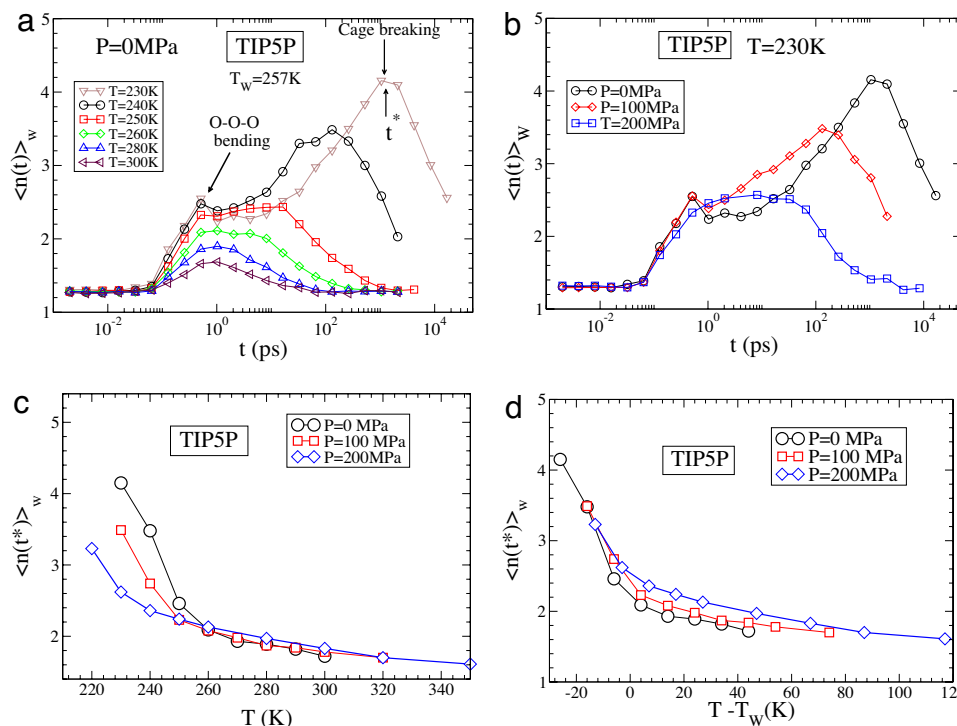
Fig. 4. Pressure and temperature dependence of clusters ("dynamic heterogeneities") that form at low temperatures and become more pronounced as the Widom line is approached. Mobile particle cluster size $\langle n(t) \rangle_w$ for different T at $P = 0$ MPa (a) and different P at $T = 230$ K (b). (c) $\langle n(t^*) \rangle_w$ for $P = 0$, 100, and 200 MPa. (d) $\langle n(t^*) \rangle_w$ as a function of $T - T_W(P)$ for three different P. All these plots are for the TIP5P model.

We see that both τ_α and D for the TIP5P (Fig. 2) display rapid changes at low T.

Fig. 3a shows $D\tau_\alpha/T$ as a function of T for the TIP5P model. At high T, $D\tau_\alpha/T$ remains approximately constant (42). At low T, $D\tau_\alpha/T$ increases, indicating a breakdown of the SE relation (1), which occurs in the same T region near the Widom line $T_W(P)$. To test whether there is a correlation between the SE breakdown and $T_W(P)$, we plot $D\tau_\alpha/T$ against $T - T_W(P)$ (Fig. 3b) and find the unexpected result that all of the curves for different pressures overlap within the limits of our accuracy for the TIP5P model. Hence, $D\tau_\alpha/T$ is a function only of $T - T_W(P)$, from which it follows that the locus of the temperature of the breakdown of the SE relation is correlated with $T_W(P)$.

Because we find a correlation between $T_W(P)$ and the breakdown of the SE relation, the hypothesized connection between the SE breakdown and the onset of dynamical heterogeneities (DH) suggests a connection between $T_W(P)$ and the onset of DH. To investigate the behavior of the dynamic heterogeneities, we study the clusters formed by the 7% most mobile molecules (43), defined as molecules with the largest displacements during a certain interval of time t. The clusters of the highly mobile molecules are defined as follows. If in a pair of mobile molecules determined in the interval $[t_0, t_0 + t]$, two oxygens at time t_0 are separated by less than the distance corresponding to position of the first minimum in the pair correlation function (0.315 nm in TIP5P and 0.350 nm in ST2), this pair belongs to the same cluster.

The weight-averaged mean cluster size

$$\langle n(t) \rangle_w \equiv \frac{\langle n^2(t) \rangle}{\langle n(t) \rangle}, \qquad [5]$$

measures the average cluster size to which a randomly chosen molecule belongs, where $\langle n(t) \rangle$ is the number-averaged mean cluster size. We show $\langle n(t) \rangle_w$ in Fig. 4 for TIP5P as a function of

observation time interval t for different T at $P = 0$ MPa (Fig. 4a). The behavior at higher P is qualitatively the same (Fig. 4b). At low T, $\langle n(t) \rangle_w$ has a maximum at the time t^* associated with the breaking of the cage formed by the neighboring molecules (see (44) and the references therein). Both the magnitude and the time scale t^* of the peak grow as T decreases. At high T, this peak merges and becomes indistinguishable from a second peak with fixed characteristic time ≈ 0.5 ps. By evaluating the vibrational density of states, we associate this feature with a low frequency vibrational motion of the system, probably the O–O–O bending mode (45).

To probe the temperature dependence of $\langle n(t) \rangle_w$, we plot the peak value $\langle n(t^*) \rangle_w$ in Fig. 4c as a function of T for $P = 0$, 100, and 200 MPa for the TIP5P model. At high T, $\langle n(t^*) \rangle_w$ is nearly constant, because at high T, clusters result simply from random motion of the molecules. Upon cooling near the Widom line, $\langle n(t^*) \rangle_w$ increases sharply. When $\langle n(t^*) \rangle_w$ is plotted as a function of $T - T_W(P)$ (see Fig. 4d), we find that (similar to the behavior of $D\tau_\alpha/T$) the three curves for $P = 0$, 100, and 200 MPa overlap, and it is apparent that the pronounced increase in $\langle n(t^*) \rangle_w$ occurs for $T \approx T_W(P)$.

Finally, we consider the correspondence between DH and static structural heterogeneity in the supercritical region; this region is characterized by large fluctuations spanning a wide range of structures, from HDL-like to LDL-like. To quantify these structural fluctuations, we calculate for the TIP5P model the temperature derivative of a local tetrahedral order parameter Q (46). In Fig. 5, we show $|(\partial Q/\partial T)_P|$ at different T for $P = 0$, 100, and 200 MPa, and find maxima (10) at $T_W(P)$ (7, 47). The maxima in $|(\partial Q/\partial T)_P|$ indicates that the change in local tetrahedrality is maximal at $T_W(P)$, which should occur when the structural fluctuations of LDL-like and HDL-like components is largest. We see that the growth of the dynamic heterogeneity coincides with the maximum in fluctuation of the local environment. Also, because Q quantifies the orientational order, the fact
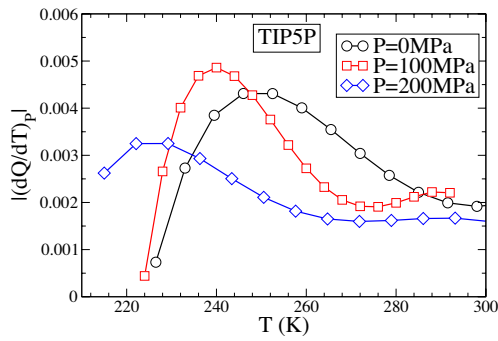
Fig. 5. $|(\partial Q/\partial T)_P|$ as a function of T for $P = 0$, 100, and 200 MPa. We note that, although the temperature of the maximum decreases with increasing pressure, the value $|(\partial Q/\partial T)_P|$ at the maximum for $P = 200$ MPa is lower than at lower pressures.

Fig. 7. Locus in P–T plane of C_P^{max} and crossover temperature $T_\times(P)$ for the ST2 model. Filled circle denotes the liquid–liquid critical point (T_C, P_C) in the ST2 model (41). The behavior of $T_\times(P)$ changes dramatically below P_C, suggesting a correlation beween the Widom line and the breakdown of the SE relation for $P < P_C$. $T_\times(P)$ for $P > P_C$ is shown in dotted line.

that we find that $|(\partial Q/\partial T)_P|$ has a maximum at approximately the same temperature where $C_P = T(\partial S/\partial T)_P$ has a maximum, supports the idea that water anomalies are closely related to the orientational order present in water.

To further test whether the breakdown of the SE relation in water is associated with the Widom line, we study another model of water, ST2, which displays a LL phase transition at low temperatures (6). Fig. 6a shows $D\tau_\alpha/T$ as a function of T for the ST2 model. At high T, $D\tau_\alpha/T$ remains approximately constant. At low T, $D\tau_\alpha/T$ increases, indicating a breakdown of the SE relation (2), which, similar to the case for the TIP5P model, occurs near the Widom line $T_W(P)$. For $P < P_C$, we plot $D\tau_\alpha/T$ against $T -$
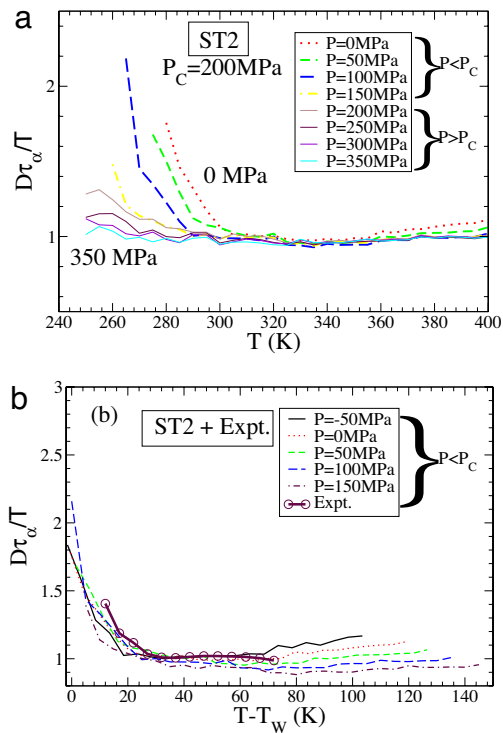
$T_W(P)$ (Fig. 6b) and we again find, similar to the TIP5P model, all of the curves for different pressures overlap within the limits of accuracy, suggesting that $D\tau_\alpha/T$ is a function only of $T - T_W(P)$.

To alternatively quantify the temperature where the SE relation breaks down, we use the observation that by plotting parametrically $\log D$ as a function of $\log(\tau_\alpha/T)$, one can identify the crossover temperature $T_\times(P)$ between the two regions by the intersection of the high T SE behavior and the low T "fractional SE behavior" $D(\tau_\alpha/T)^\xi = $ const (19, 40). Fig. 7 shows the locus

a

b

Fig. 6. Test for the ST2 model that the SE breakdown is correlated with crossing the Widom line at low pressures. (*a*) Analog of Fig. 3*a* for the ST2 model. The data for $P > P_C$ are shown using thick dotted and dashed curves, whereas the data for $P > P_C$ are shown in thin curves. For all panels, $D\tau_\alpha/T$ is scaled by its high T value to facilitate comparison of the different systems. (*b*) Analog of Fig. 3*b* for the ST2 model including the experimental data of $D\eta/T$ (15, 48–50).
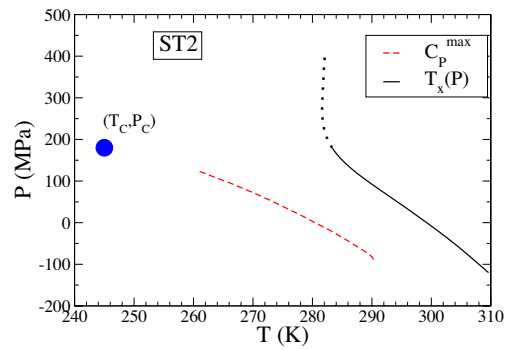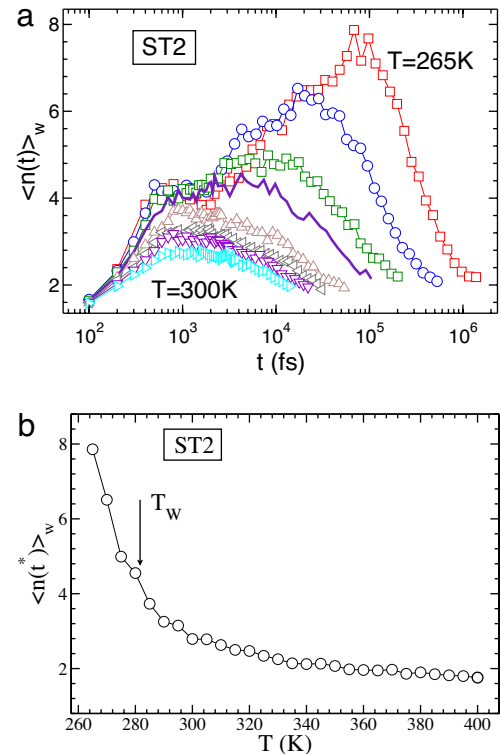

a

b

Fig. 8. Dynamic heterogeneities in the ST2 model of water. (*a*) $\langle n(t) \rangle_w$ as a function of t at 5 K intervals for $\rho = 0.83$ g/cm^3 from 265 to 300 K. The bold line shows the $T = 280$ K isotherm where the constant volume specific heat C_V has a maximum. (*b*) $\langle n(t^*) \rangle_w$ as a function of T for $\rho = 0.83$ g/cm^3. We indicate the temperature at which C_V has a maximum by a vertical arrow. The maximum of C_V occurs in the same region where other response functions, such as C_P, have maxima.

of $T_\times$ in the P–T plane of the ST2 model. We confirm that the same collapse of $D\tau_\alpha/T$ can be found by replacing T with $T - T_\times(P)$, demonstrating (Fig. 7) that the locus of SE breakdown defined by $T_\times(P)$ approximately tracks $T_W(P)$ for $P < P_C$. For $P > P_C$, there is no Widom line and we can see the drastic behavior change of $T_\times(P)$, which supports the hypothesis that the SE relation breakdown is correlated to the LL phase transition. There is also some difference between the ST2 and TIP5P models in the relative location of the breakdown of the SE relation and $T_W(P)$, evidenced by the fact that the magnitude of the SE breakdown is different for ST2 at $T = T_W(P)$. As a result, the results for the two models will not collapse when plotted together. Moreover, we find that $D\eta/T$ from the experimental data plotted against $T - T_W(P)$ (Fig. 6b), coincide with the ST2 results, suggesting that the data collapse likely exists for water when T is replaced by $T - T_W(P)$. The experimental data for D were taken from ref. 15, and the experimental data for η were taken from refs. 48–50. The T_W for water at $P = 1$ atm is taken to be the temperature of the C_p^{max} which is ≈ 225 K (11, 47). For $P > P_C$ (when there is no Widom line), water behaves similar to simple glass forming liquids, and so we expect the breakdown of the SE relation for water to be similar to other simple liquids. Specifically, the SE relation is believed to break down at $T \approx (1.2–1.6)T_g$ (19), roughly coinciding with the temperature $T_{MCT}(P)$, where the mode coupling description of the dynamics fails (19, 35). This has been verified for the SPC/E model of water (51), and we expect the same is true for the ST2 and TIP5P models.

To test whether there is an increase in dynamic heterogeneities at $T_W(P)$ as found for the TIP5P, we show $\langle n(t)\rangle_w$ for different T along an isochore of density $\rho = 0.83$ g/cm³ for the ST2 model in Fig. 8a. We show an isochore because only isochoric data are available from ref. 41. As in the case of TIP5P, we find the emergence of a second time scale larger than 0.5 ps in $\langle n(t)\rangle_w$ near

the crossing of the Widom line. Similarly, $\langle n(t^*)\rangle_w$ increases near the Widom line temperature (see Fig. 8b). Hence, the sharp growth of DH and the appearance of a second time scale in $\langle n(t)\rangle_w$ both occur near the Widom line. We also find that the magnitude of $\langle n(t^*)\rangle_w$ is larger for the ST2 model than for the TIP5P model at $T_W(P)$, consistent with the above observation that the breakdown of the SE relation is more pronounced for the ST2 model than for the TIP5P model.

Discussion and Summary

We have shown that the breakdown of the SE relation for $P < P_C$ can be correlated with the Widom line emanating from the LL critical point. In particular, rescaling T by $T - T_W(P)$ yields data collapse of $D\tau_\alpha/T$ for different pressures. Rapid structural changes occur for T near $T_W(P)$, where larger LDL "patches" emerge upon cooling (52–54). The size of the dynamic heterogeneities also increases sharply as the Widom line is crossed. The breakdown of the SE relation can be understood by the fact that diffusion at low T is dominated by regions of fastest moving molecules (DH), whereas the relaxation of the system as a whole is dominated by the slowest moving molecules. Consistent with this, we find that the growth of mobile particle clusters occurs near the Widom line and also near the breakdown of the SE relation for $P < P_C$. Thus, the SE breakdown and sharp growth in dynamic heterogeneities in water are consistent with the LL critical point hypothesis (2–6). Our results are also consistent with recent experimental findings in confined water (8, 13, 14).

1. Waller R, trans (1684) *Essayes of Natural Experiments* (Johnson Reprint Corporation, New York, 1964), facsimile.
2. Mishima O, Stanley HE (1998) *Nature* 392:164–168.
3. Debenedetti PG, Stanley HE (2003) *Physics Today* 56:40–46.
4. Debenedetti PG (2003) *J Phys Condens Matter* 15:R1669–R1726.
5. Angell CA (2004) *Annu Rev Phys Chem* 55:559–583.
6. Poole PH, Sciortino F, Essmann U, Stanley HE (1992) *Nature* 360:324–328.
7. Xu L, Kumar P, Buldyrev SV, Chen S-H, Poole PH, Sciortino F, Stanley HE (2005) *Proc Natl Acad Sci USA* 102:16558–16562.
8. Liu L, Chen S-H, Faraone A, Yen C-W, Mou C-Y (2005) *Phys Rev Lett* 95:117802.
9. Kumar P, Franzese G, Stanley HE (2007) http://arxiv.org/abs/cond-mat/0702108.
10. Kumar P, Yan Z, Xu L, Mazza M, Buldyrev SV, Chen S-H, Sastry S, Stanley HE (2006) *Phys Rev Lett* 97:177802.
11. Starr FW, Angell A, Stanley HE (2003) *Physica A* 323:51–66.
12. Starr FW, Sciortino F, Stanley HE (1999) *Phys Rev E* 60:6757–6768.
13. Mallamace F, Broccio M, Corsaro C, Faraone A, Wanderlingh U, Liu L, Mou C-Y, Chen S-H (2006) *J Chem Phys* 124:161102.
14. Chen S-H, Mallamace F, Mou, C.-Y, Broccio M, Corsaro C, Faraone A, Liu L (2006) *Proc Natl Acad Sci USA* 103:12974–12978.
15. Prielmeier FX, Lang EW, Speedy RJ, Lüdemann HD (1987) *Phys Rev Lett* 59:1128–1131.
16. Egelstaff PA (1994) *An Introduction to the Liquid State* (Clarendon, New York).
17. Jonas J, Akai JA (1977) *J Phys Chem* 66:4946–4950.
18. Keyes T, Oppenheim I (1973) *Phys Rev A* 8:937–949.
19. Sillescu H (1999) *J Non-Cryst Solids* 243:81–108.
20. Cicerone MT, Blackburn FR, Ediger MD (1995) *Macromolecules* 28:8224–8232.
21. Cicerone MT, Ediger MD (1995) *J Chem Phys* 103:5683–5692.
22. Berthier L, Biroli G, Bouchaud J-P, Cipelletti L, El Masri D, L'Hote D, Ladieu D, Pierno M (2005) *Science* 310:1797–1800.
23. Pollack GL (1981) *Phys Rev A* 23:2660–2663.
24. Pollack GL, Enyeart JJ (1985) *Phys Rev A* 31:980–984.
25. Ediger MD (2005) *Annu Rev Phys Chem* 51:99–128.
26. Fujara F, Geil B, Sillescu H, Fleischer G, (1992) *Z Phys B* 88:195–204.
27. Cicerone MT, Blackburn FR, Ediger MD (2005) *J Chem Phys* 102:471–479.
28. Ehlich D, Sillescu H (1990) *Macromolecules* 23:1600.
29. Kumar P (2006) *Proc Natl Acad Sci USA* 103:12955–12956.
30. Stillinger FH, Hodgon JA (1994) *Phys Rev E* 50:2064.
31. Gilles T, Kivelson D (1995) *J Chem Phys* 103:3071–3073.
32. Ngai KL (1999) *Phil Mag B* 79:1783–1797.
33. Weeks ER, Crocker JC, Levitt AC, Schofield A, Weitz DA (2000) *Science* 287:627–631.
34. Kanno H, Angell CA (1979) *J Chem Phys* 70:4008–4016.
35. Rössler E (1990) *Phys Rev Lett* 65:1595–1598.
36. Mahoney MW, Jorgensen WL (2000) *J Chem Phys* 112:8910–8922.
37. Yamada M, Mossa S, Stanley HE, Sciortino F (2002) *Phys Rev Lett* 88:195701.
38. Paschek D (2005) *Phys Rev Lett* 94:217802.
39. Stillinger FH, Rahman A (1974) *J Chem Phys* 60:1545.
40. Becker SR, Poole PH, Starr FW (2006) *Phys Rev Lett* 97:055901.
41. Poole PH, Saika-Voivod I, Sciortino F (2005) *J Phys Condens Matter* 17:L431–L437.
42. Netz PA, Starr FW, Barbosa MC, Stanley HE (2002) *J Mol Liquids* 101:159–168.
43. Donati C, Glotzer SC, Poole PH, Kob W, Plimpton SJ (1999) *Phys Rev E* 60:3107–3119.
44. Giovambattista N, Buldyrev SV, Stanley HE, Starr FW (2005) *Phys Rev E* 72:011202.
45. Tsai KH, Wu T-M (2005) *Chem Phys Lett* 417:390–395.
46. Errington JR, Debenedetti PG (2001) *Nature* 409:318–321.
47. Maruyama S, Wakabayashi K, Oguni M (2004) *AIP Conf Proc* 708:675–676.
48. Hallet J (1963) *Proc Phys Soc* 82:1046–1050.
49. Opisov YA, Zheleznyi BV, Bondarenko NF (1977) *J Phys Chem* 51:748–752.
50. Angell A (1981) in *Water: A Comprehensive Treatise*, ed Franks F (Plenum, New York).
51. Starr FW, Harrington S, Sciortino F, Stanley HE (1999) *Phys Rev Lett* 82:3629–3632.
52. Errington JR, Debenedetti PG, Torquato S (2002) *Phys Rev Lett* 89:215503.
53. Stanley HE, Teixeira J (1980) *J Chem Phys* 73:3404–3422.
54. Geiger A, Stanley HE (1982) *Phys Rev Lett* 49:1749–1752.

CHEMISTRY

APPLIED PHYSICAL SCIENCES